Integration of Photoacoustic and Ultrasound Computed Tomography

Thomas P. Matthews and Mark A. Anastasio

Department of Biomedical Engineering

Washington University in St. Louis

Outline

- Overview
- Photoacoustic Computed Tomography (PACT)
- Ultrasound Computed Tomography (USCT)
- Joint Reconstruction for PACT
- Joint Reconstruction for PACT and USCT

Photoacoustic computed tomography (PACT)

- PACT holds great potential for human and animal imaging (here, we focus on human breast imaging)

- PACT is a hybrid imaging modality.
  - » Utilizes optical radiation to interrogate the object, but ultrasound detection principles
  - » Measures absorbed optical energy within tissue

- PACT methods have
  - » Strong (hemoglobin-based) contrast similar to pure optical methods
  - » High spatial resolution similar to pure ultrasonic methods

- Endogenous hemoglobin-based contrast can be exploited to
  - » Image anatomical structures
  - » Serve as a functional contrast for imaging of oxygen saturation (sO_2).

Imaging physics & data acquisition for PACT

- A variety of PACT imaging systems have been developed.
- The acquisition process generally contains the following steps:
  - » An optical pulse is employed to illuminate the breast
  - » Absorbed light gives rise to an initial pressure distribution via the photoacoustic effect
  - » Pressure propagates outward based on the acoustic properties of the medium
  - » All transducers (receivers) measure the resultant wavefield data.

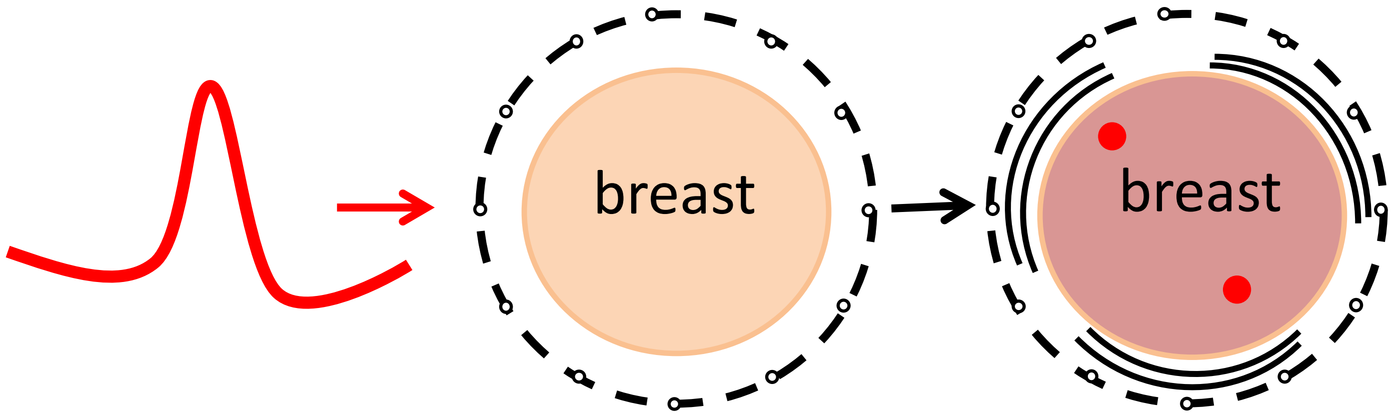

- <u>Goal:</u> To reconstruct the initial pressure distribution from the measured wavefield data.

Ultrasound computed tomography (USCT)

- USCT is based on the transmission of ultrasonic energy through an object, rather than reflection at an interface like conventional B-mode ultrasound.

- Advantages of USCT for breast imaging
  - » Radiation-free
  - » Breast-compression-free
  - » Relatively inexpensive
  - » Large field-of-view
  - » Performance largely operator-independent

- Contrast mechanisms
  - » Acoustic reflectivity
  - » Acoustic attenuation
  - » <u>Speed-of-sound (SOS)</u>

Washington University in St. Louis
School of Engineering & Applied Science

Imaging physics & data acquisition for USCT

- A variety of USCT imaging systems have been developed.
- One single shot:
  - » A transducer (emitter) generates an acoustic pulse to insonify a breast.
  - » All transducers (receivers) measure the resultant wavefield data.
- One data set contains V single shots.

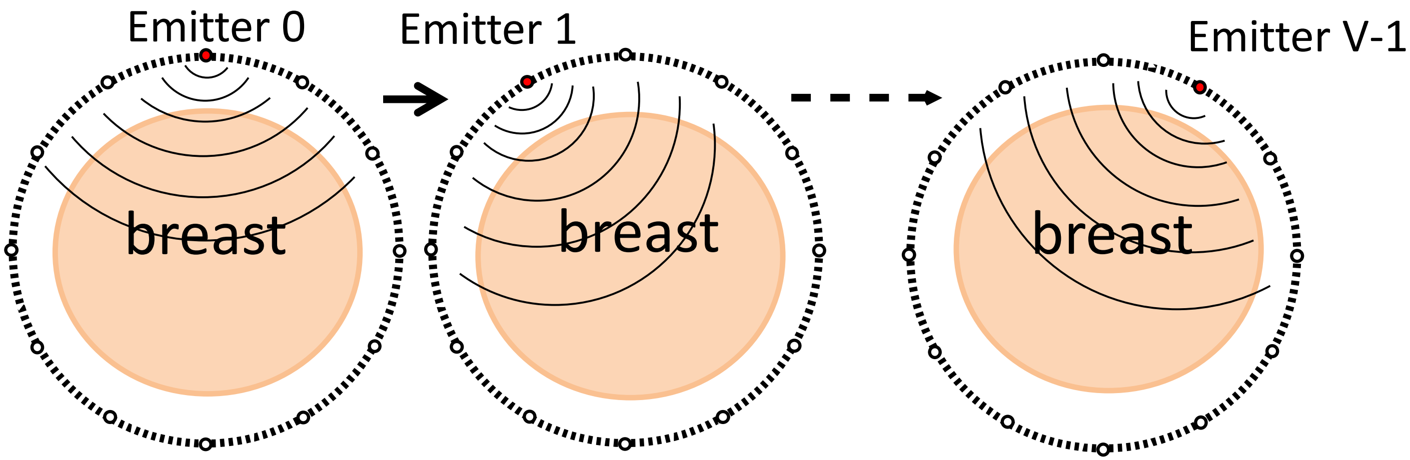

- <u>Goal:</u> To reconstruct the breast sound speed distribution from the measured wavefield data.

Washington University in St. Louis
School of Engineering & Applied Science

Benefits of combined system

- Shared detection hardware
- Complementary tissue contrasts
- Automatically co-registered images
- Ability to correct for sound speed variations in PACT image reconstruction

Optimization-based image reconstruction

- Flexible approach that can be utilized to accurately model the underlying imaging physics
- Can reconstruct image by (approximately) inverting imaging model
- Often too computationally burdensome to invert or compute pseudo-inverse of our imaging model directly
- Instead, we solve an optimization problem that balances
  - » Matching the measured data with simulated data obtained by use of our model
  - » A priori knowledge about the objects being measured

Outline

- Overview
- Photoacoustic Computed Tomography (PACT)
- Ultrasound Computed Tomography (USCT)
- Joint Reconstruction for PACT
- Joint Reconstruction for PACT and USCT

Full-wave equation model for PACT

- Time-domain wave equation (constant density & lossless medium)

$$\nabla^2 \underbrace{p}_{\text{Pressure}}(\mathrm{r},\mathrm{t}) - \frac{1}{\underbrace{c}_{\text{Sound speed}}{}^2(r)}\frac{\partial^2}{\partial t^2}p(r,t) = 0$$

$$p(r,0) = p_0(r) \qquad \frac{\partial}{\partial t}p(r,0) = 0$$

- Numerical wave equation solver (solved by k-space pseudo-spectral method [Tabei 2002])

$$\underbrace{\boldsymbol{g}_{PA}}_{\text{Measured data vector}} = \underbrace{\boldsymbol{M}}_{\text{Sampling matrix}}\underbrace{\boldsymbol{H}_{PA}(\boldsymbol{c})}_{\text{Wave solver (c-dependent)}}\underbrace{\boldsymbol{p}_0}_{\text{Sought-after Initial pressure}}$$

Discrete-to-discrete Imaging model

Inverse problem formulation for initial pressure (PACT)

- Formulation of a minimization problem:

$$\widehat{\boldsymbol{p_0}} = \underset{\boldsymbol{p_0}}{\operatorname{argmin}}\, \underbrace{F_{PA}}_{\text{Data fidelity}}(\boldsymbol{p_0}, \boldsymbol{c}) + \lambda \underbrace{R_p}_{\text{Penalty}}(\boldsymbol{p_0})$$

where

$$\underbrace{F_{PA}}_{\substack{\text{Convex w.r.t. } p_0, \\ \text{Differentiable}}}(\boldsymbol{p_0}, \boldsymbol{c}) = \frac{1}{2} \left\| \underbrace{\underline{\boldsymbol{g}_{PA}}}_{\text{Measurements}} - \boldsymbol{M}\boldsymbol{H}_{PA}(\boldsymbol{c})\boldsymbol{p_0} \right\|_2^2$$

$$\underbrace{R_p}_{\text{Convex, Non-smooth}}(\boldsymbol{p_0}) = \|\boldsymbol{\nabla} \boldsymbol{p_0}\|_{\mathbf{1}}$$

- Optimization problem is solved by use of the Fast Iterative Shrinkage Thresholding Algorithm (FISTA) [Beck & Teboulle 2009, Huang et al. 2003]

Computer-simulation studies

- Numerical breast phantom, segmented and extracted from clinical MRI breast measurements [Lou 2016]

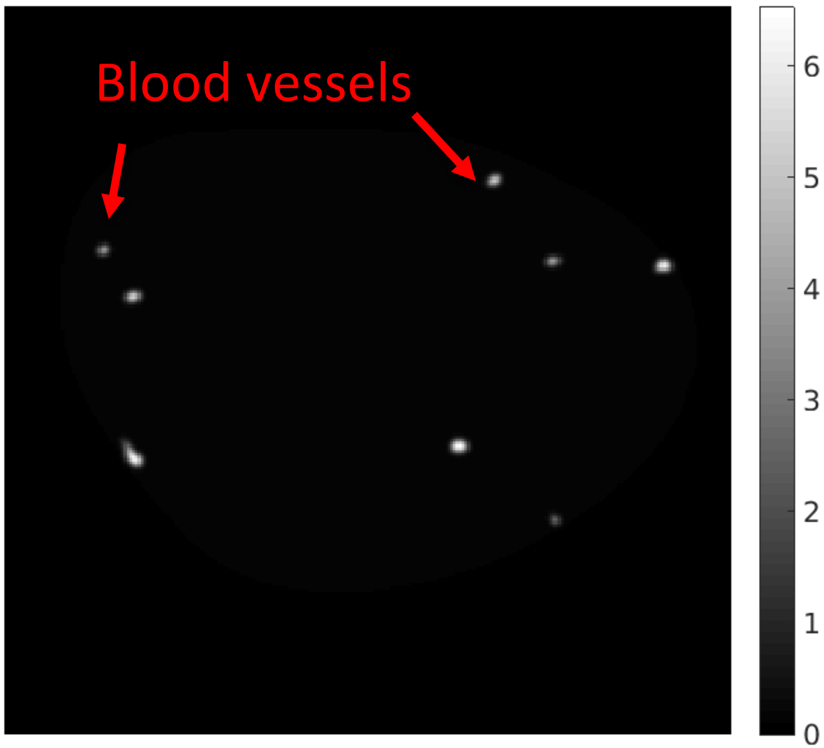

Initial pressure distribution [A.U.]

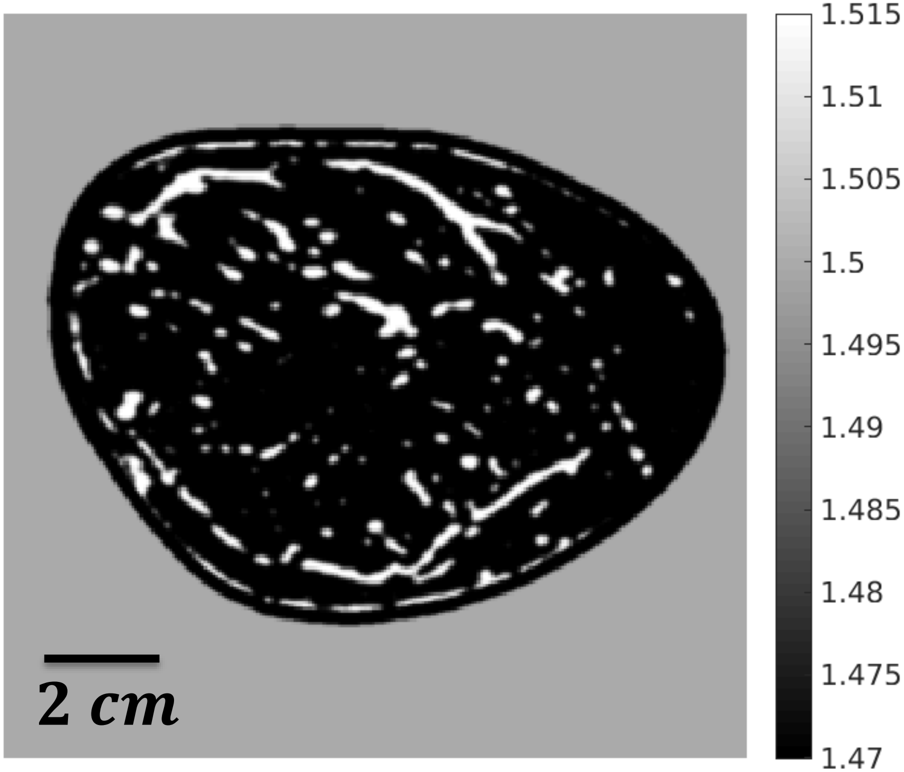

Sound speed distribution [mm/μs]

Washington University in St. Louis
SCHOOL OF ENGINEERING & APPLIED SCIENCE

Computer-simulation studies

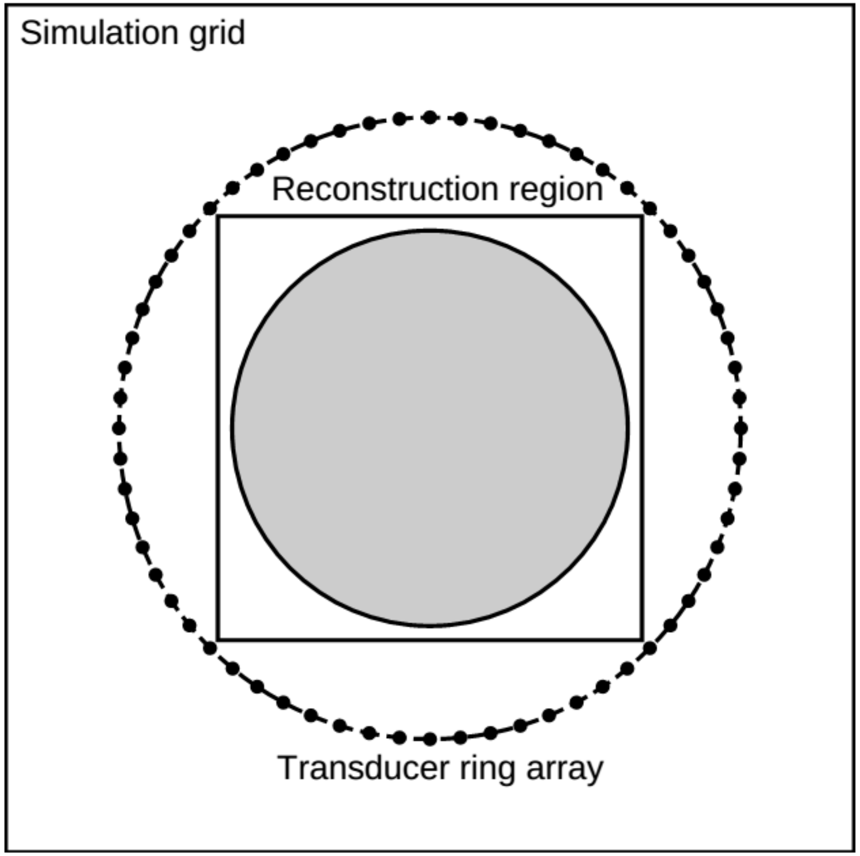

Simulation of pressure

- Grid points: 2048 x 2048
- Pixel size: 0.125 mm
- Number of time points: 7000
- Time step: 0.025 µs (f_s = 40 MHz)

Reconstruction

- Grid points: 1024 x 1024
- Pixel size: 0.25 mm
- Number of time points: 3500
- Time step: 0.05 µs (f_s = 20 MHz)

Number of transducers: 512
Radius of transducer array: 110 mm

No noise added

Reconstructed initial pressure distribution

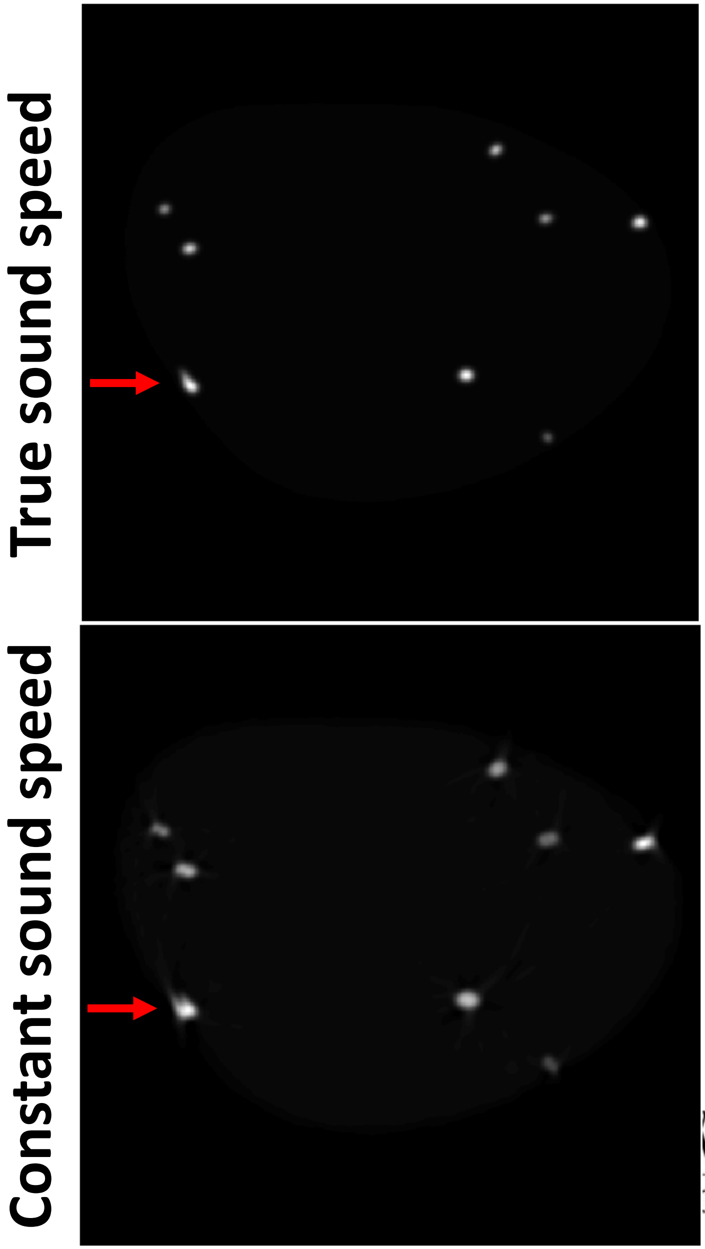

Ignoring sound speed variations can result in significant errors in the reconstructed initial pressure distribution.

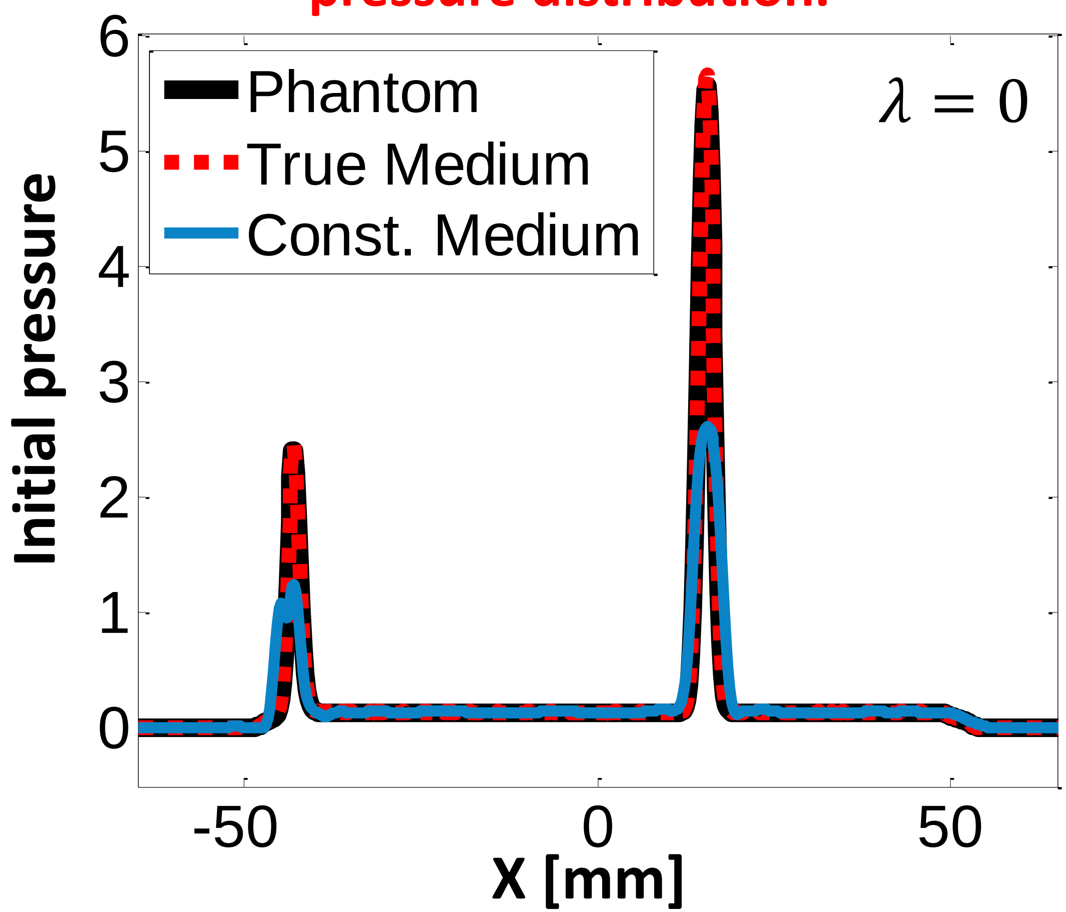

Washington University in St.Louis
School of Engineering & Applied Science

Inverse problem formulation for sound speed (PACT)

- Formulation of a minimization problem:

$$\hat{\boldsymbol{c}} = \underset{\boldsymbol{c}}{\operatorname{argmin}} \underbrace{F_{PA}}_{\text{Data fidelity}}(\boldsymbol{p_0}, \boldsymbol{c}) + \lambda \underbrace{R_c}_{\text{Penalty}}(\boldsymbol{c})$$

where

$$\underbrace{F_{PA}(\boldsymbol{p_0}, \boldsymbol{c})}_{\text{Non-convex w.r.t. c, Differentiable}} = \frac{1}{2}\left\| \underbrace{\boldsymbol{g}_{PA}}_{\text{Measurements}} - \boldsymbol{MH}_{PA}(\boldsymbol{c})\boldsymbol{p_0} \right\|_2^2$$

$$\underbrace{R_c(\boldsymbol{c})}_{\text{Convex, Smooth}} = \sqrt{\epsilon + \|\boldsymbol{\nabla c}\|_2^2}$$

- Optimization problem is solved by use of the L-BFGS algorithm[Nocedal 1980]

Washington University in St. Louis
School of Engineering & Applied Science

Reconstructed sound speed distribution (PACT)

The reconstructed sound speed is very sensitive to errors in the initial pressure distribution.

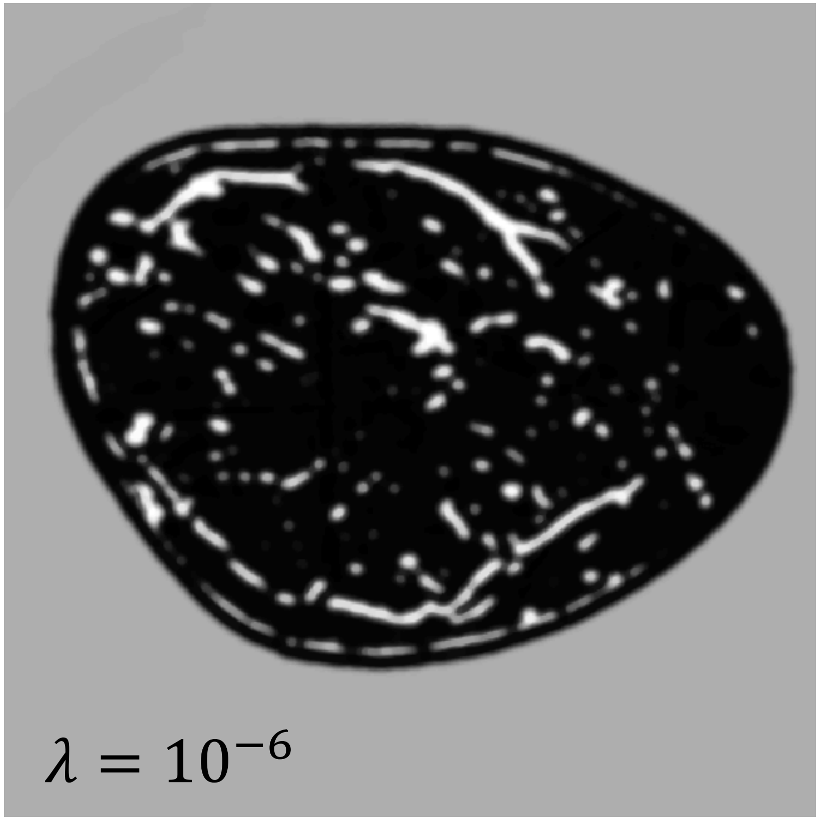

True initial pressure

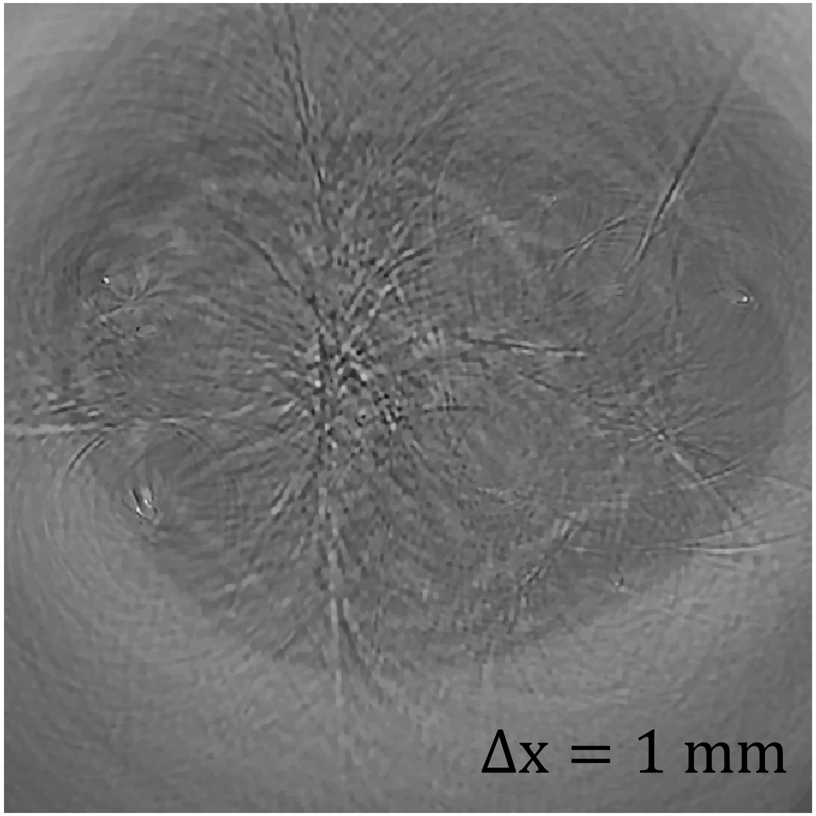

Shifted initial pressure

Washington University in St. Louis
School of Engineering & Applied Science

Outline

- Overview
- Photoacoustic Computed Tomography (PACT)
- Ultrasound Computed Tomography (USCT)
- Joint Reconstruction for PACT
- Joint Reconstruction for PACT and USCT

Full-wave equation model for USCT

- Time-domain wave equation (constant density & lossless medium)

$$\nabla^2 p_v(r,t) - \frac{1}{c^2(r)}\frac{\partial^2}{\partial t^2} p_v(r,t) = -4\pi s_v(r,t)$$

Pressure at *v*-th view

Source for *v*-th view

$$p_v(r,0) = 0 \qquad \frac{\partial}{\partial t} p_v(r,0) = 0$$

- Numerical wave equation solver (solved by k-space pseudo-spectral method [Tabei 2002])

$$\boldsymbol{g}_v = \boldsymbol{M}\boldsymbol{H}_{US}(\boldsymbol{c})\boldsymbol{s}_v$$

Measured data vector

Sampling matrix

Wave solver (c-dependent)

Standard waveform inversion problem formulation

- Formulation of a minimization problem:

$$\hat{\boldsymbol{c}} = \underset{\boldsymbol{c}}{\operatorname{argmin}} \underbrace{F_{US}}_{\text{Data fidelity}}(\boldsymbol{c}) + \lambda \underbrace{R_c}_{\text{Penalty}}(\boldsymbol{c})$$

- Data fidelity term:

$$F_{US}(\boldsymbol{c}) = \frac{1}{2} \sum_{v=0}^{V-1} \left\| \underbrace{\boldsymbol{g}_v}_{\text{Measurements}} - \boldsymbol{M}\boldsymbol{H}_{US}(\boldsymbol{c})\boldsymbol{s}_v \right\|_2^2$$

Non-convex w.r.t. c,
Differentiable

» V: number of emitters

Waveform inversion with source encoding (WISE)

- Choose some random encoding vector w with which to encode the sources and measured data

$$\underline{\boldsymbol{g}_{\boldsymbol{w}}} = \sum_{v=0}^{V-1} \underline{[\boldsymbol{w}]}_v \, \underline{\boldsymbol{g}_v} \qquad \boldsymbol{s}_{\boldsymbol{w}} = \sum_{v=0}^{V-1} \underline{[\boldsymbol{w}]}_v \, \boldsymbol{s}_v$$

Encoding vector

K. Wang, et al. *IEEE UFFC* 62(3), 475-94 (2015).

- New data fidelity term

$$F_{SUS}(\boldsymbol{c}) = \underline{\boldsymbol{E}_{\boldsymbol{w}}} \left[\frac{1}{2} \left\| \underline{\boldsymbol{g}_{\boldsymbol{w}}} - \boldsymbol{M}\boldsymbol{H}_{US}(\boldsymbol{c})\boldsymbol{s}_{\boldsymbol{w}} \right\|_2^2 \right]$$

Expectation w.r.t. w

- When w has a zero mean and an identity covariance matrix,

$$F_{SUS}(\boldsymbol{c}) = F_{US}(\boldsymbol{c})$$

E. Haber et. al., SIAM J. Optimiz. 22(3), P739-757 (2012).

- Optimization problem solved by used of stochastic gradient descent

Reconstructed sound speed (Impact of number of views)

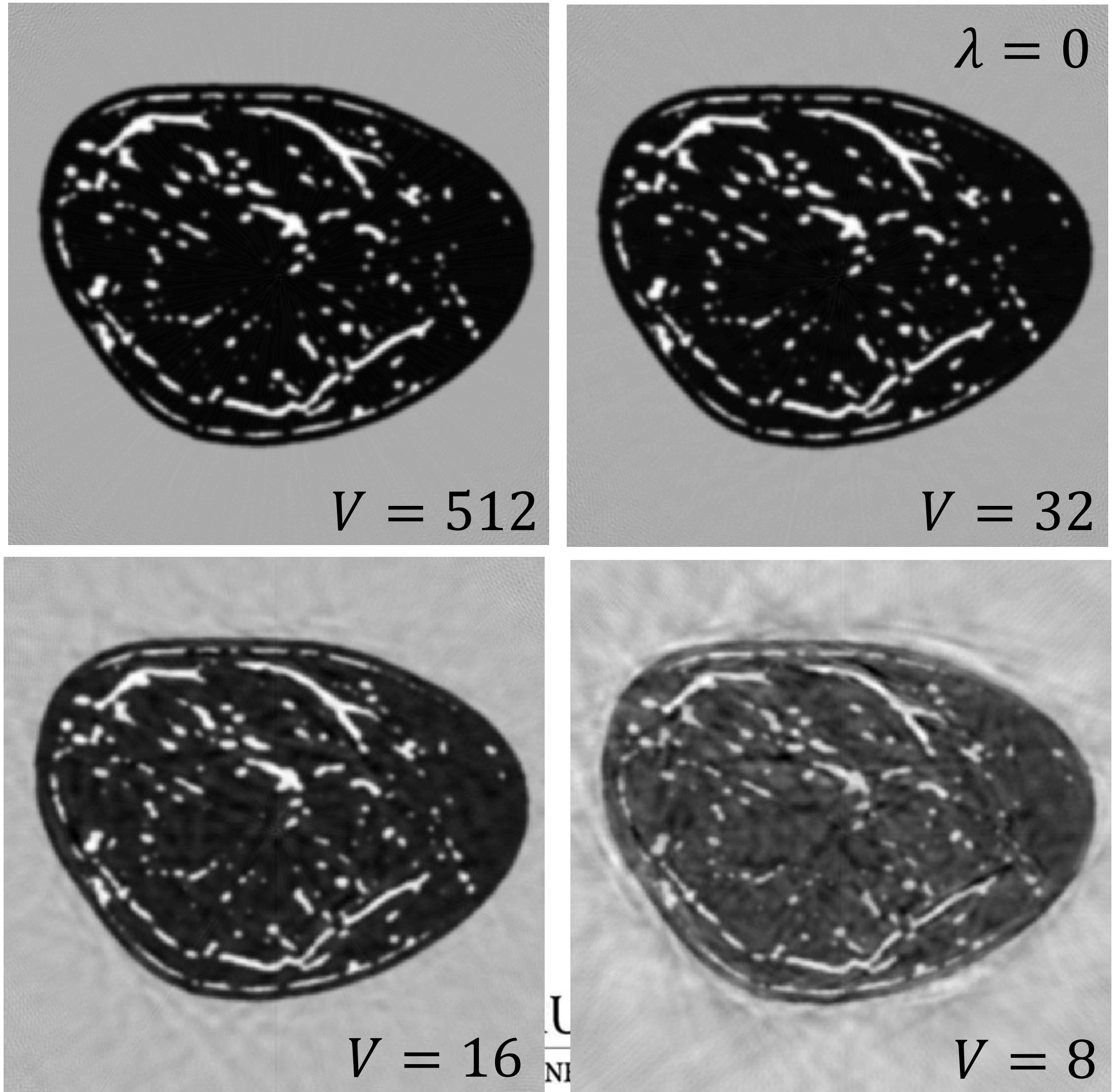

Outline

- Overview
- Photoacoustic Computed Tomography (PACT)
- Ultrasound Computed Tomography (USCT)
- Joint Reconstruction for PACT
- Joint Reconstruction for PACT and USCT

Exploiting acoustic information in PACT data

- Can jointly estimate sound speed and absorbed optical energy density from PACT measurements alone [Jiang 2006, Zhang 2008, Huang 2016]

$$\widehat{\boldsymbol{p_0}}, \hat{\boldsymbol{c}} = \underset{\boldsymbol{p_0}, \boldsymbol{c}}{\operatorname{argmin}} F_{PA}(\boldsymbol{p_0}, \boldsymbol{c}) + \lambda_1 R_p(\boldsymbol{p_0}) + \lambda_2 R_c(\boldsymbol{c})$$

- Divide objective function into two subproblems [Huang 2016]
  - » Estimate p_0 given c (convex)

$$\widehat{\boldsymbol{p_0}} = \underset{\boldsymbol{p_0}}{\operatorname{argmin}} F_{PA}(\boldsymbol{p_0}, \boldsymbol{c}) + \lambda_1 R_p(\boldsymbol{p_0})$$

  - » Estimate c given p_0 (non-convex)

$$\hat{\boldsymbol{c}} = \underset{\boldsymbol{c}}{\operatorname{argmin}} F_{PA}(\boldsymbol{p_0}, \boldsymbol{c}) + \lambda_2 R_c(\boldsymbol{c})$$

Alternating minimization

Input: $\underline{\boldsymbol{g}_{PA}}, \boldsymbol{p}_{\mathbf{0}}^{(0)}, \boldsymbol{c}^{(0)}, \lambda_1, \lambda_2$

Output: $\widehat{\boldsymbol{p}_{\mathbf{0}}}, \hat{\boldsymbol{c}}$

1: $k = 0$ {k is the iteration number}

2: $\boldsymbol{while}$ (stopping criteria not satisfied) $\boldsymbol{do}$

3: $\quad \boldsymbol{p}_{\mathbf{0}}^{(k+1)} = \underset{\boldsymbol{p}_{\mathbf{0}}}{\operatorname{argmin}} F_{PA}\left(\boldsymbol{p}_{\mathbf{0}}, \boldsymbol{c}^{(k)}\right) + \lambda_1 R_p(\boldsymbol{p}_{\mathbf{0}})$

4: $\quad \boldsymbol{c}^{(k+1)} = \underset{\boldsymbol{c}}{\operatorname{argmin}} F_{PA}\left(\boldsymbol{p}_{\mathbf{0}}^{(k+1)}, \boldsymbol{c}\right) + \lambda_2 R_c(\boldsymbol{c})$

5: $\quad k = k + 1$

6: $\boldsymbol{end\ while}$

7: $\widehat{\boldsymbol{p}_{\mathbf{0}}} = \boldsymbol{p}_{\mathbf{0}}^{(k)}$

8: $\hat{\boldsymbol{c}} = \boldsymbol{c}^{(k)}$

Washington University in St. Louis
School of Engineering & Applied Science

[Huang 2016]

Results for joint reconstruction from PACT data alone

The sound speed and initial pressure distributions cannot be stably recovered from PACT measurements alone [Stefanov and Uhlmann 2003a].

Constant sound speed initialization

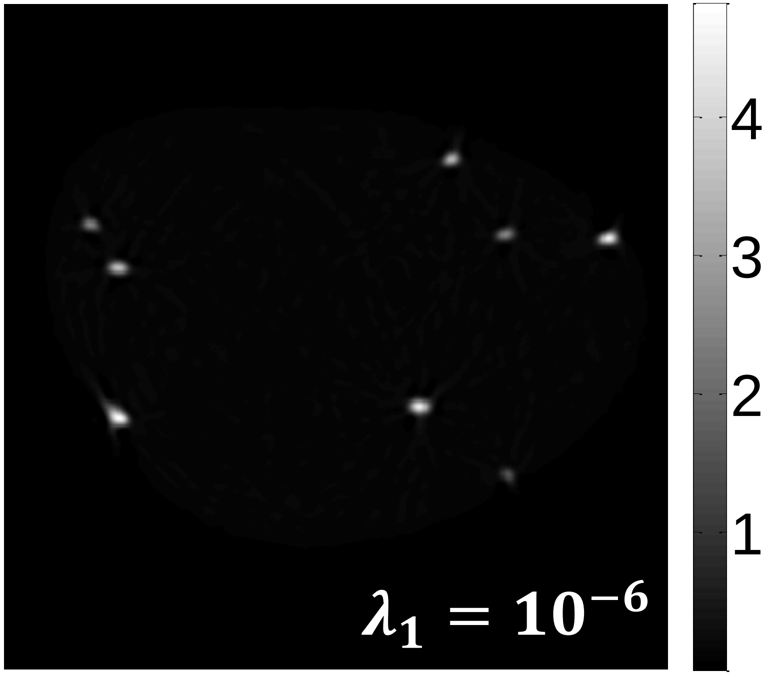

Initial pressure

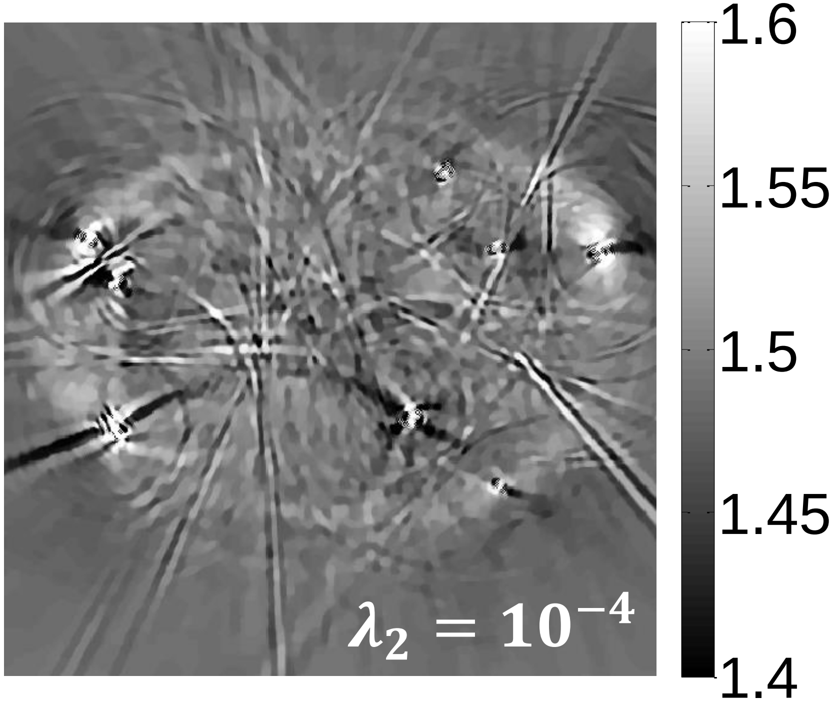

Sound speed [mm/μs]

The smoothness of the sound speed can be increased by increasing λ_2, but the sound speed is never accurately recovered.

Results for joint reconstruction from PACT data alone

Bent-ray (USCT-based) sound speed initialization

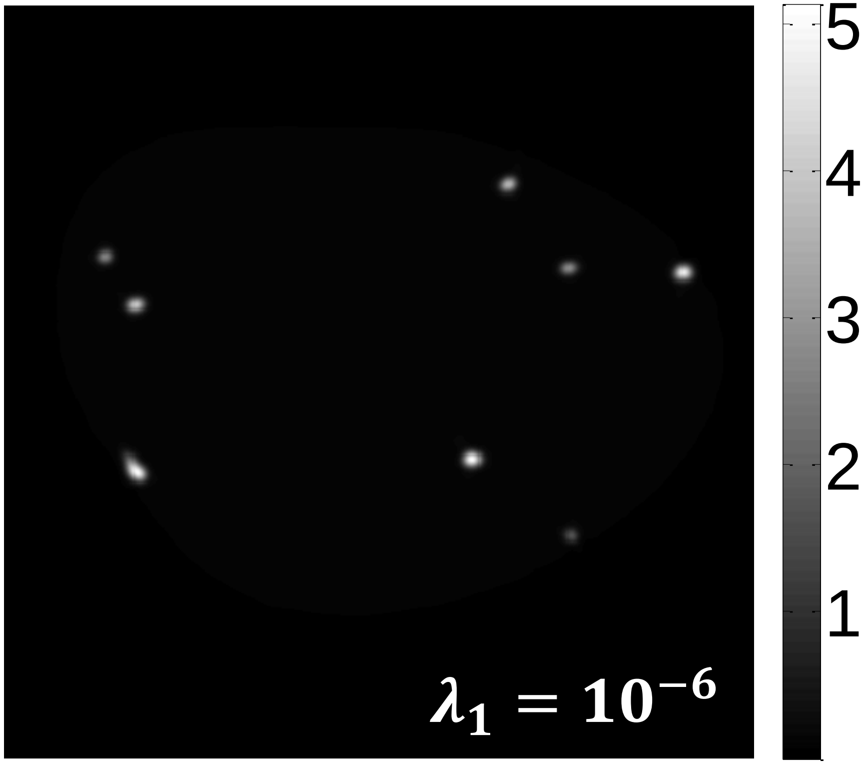

Initial pressure

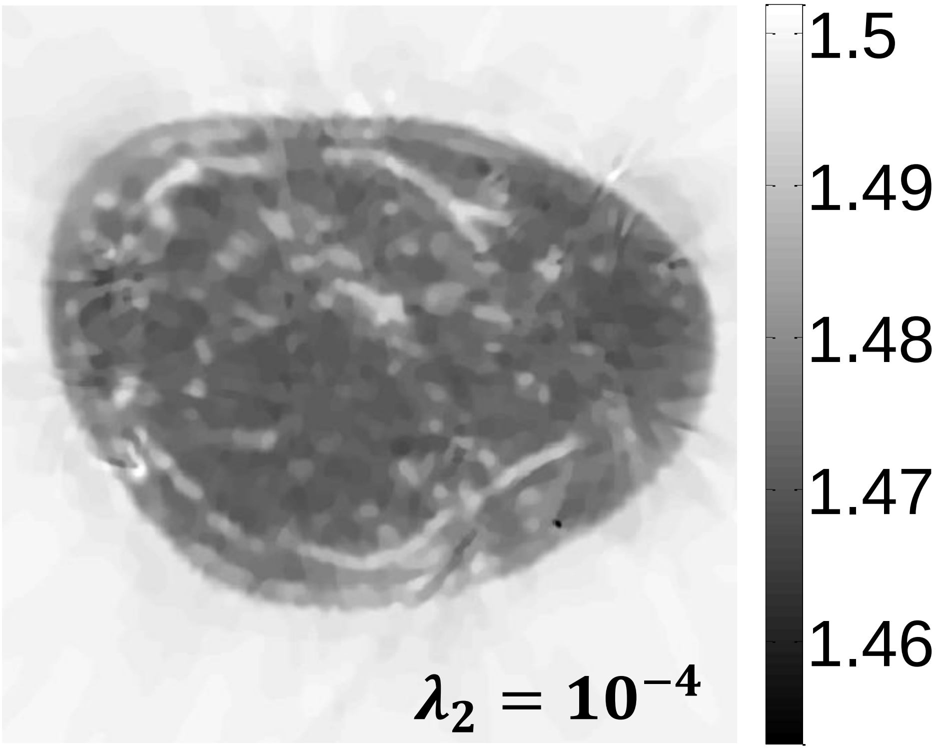

Sound speed [mm/μs]

With a good initial guess and strong regularization, the reconstructed sound speed is more accurate.

Outline

- Overview
- Photoacoustic Computed Tomography (PACT)
- Ultrasound Computed Tomography (USCT)
- Joint Reconstruction for PACT
- Joint Reconstruction for PACT and USCT

Image reconstruction for hybrid PACT/USCT systems

- Two-step conventional approach [Jin and Wang 2006, Manohar 2007, Jose 2012, Xia 2013]
  - » Estimate sound speed from USCT measurements
  - » Estimate initial pressure distribution using this sound speed map

- This approach is **not** optimal.
  - » Independent estimation of sound speed and initial pressure distributions fails to exploit acoustic information in PACT measurements.

New approach to joint reconstruction

Solution: Joint reconstruction of initial pressure and sound speed distributions from combined PACT/USCT measurements

- Automatically accounts for sound speed variations
- Exploits acoustic information presentation in the PACT measurements
- May minimize systematic artifacts by balancing errors in the imaging models
- Greater numerical stability than reconstructing from PACT data alone
- Allows reconstruction of sound speed from sparse USCT data, which could reduce acquisition times and simplify hardware designs

Optimization problem for combined measurements

- Overall optimization problem for synergistic reconstruction

$$\widehat{\boldsymbol{p_0}}, \hat{\boldsymbol{c}} = \underset{\boldsymbol{p_0}, \boldsymbol{c}}{\operatorname{argmin}} F_{PA}(\boldsymbol{p_0}, \boldsymbol{c}) + \underline{\beta} F_{SUS}(\boldsymbol{c}) + \lambda_1 R_p(\boldsymbol{p_0}) + \lambda_2 R_c(\boldsymbol{c})$$

Controls relative weight of two data fidelity terms

- New subproblem for estimating c

$$\hat{\boldsymbol{c}} = \underset{\boldsymbol{c}}{\operatorname{argmin}} F_{PA}(\boldsymbol{p_0}, \boldsymbol{c}) + \beta F_{SUS}(\boldsymbol{c}) + \lambda_2 R_c(\boldsymbol{c})$$

Washington University in St. Louis
School of Engineering & Applied Science

Results for combined joint reconstruction (16 views)

Initial pressure

Sound speed

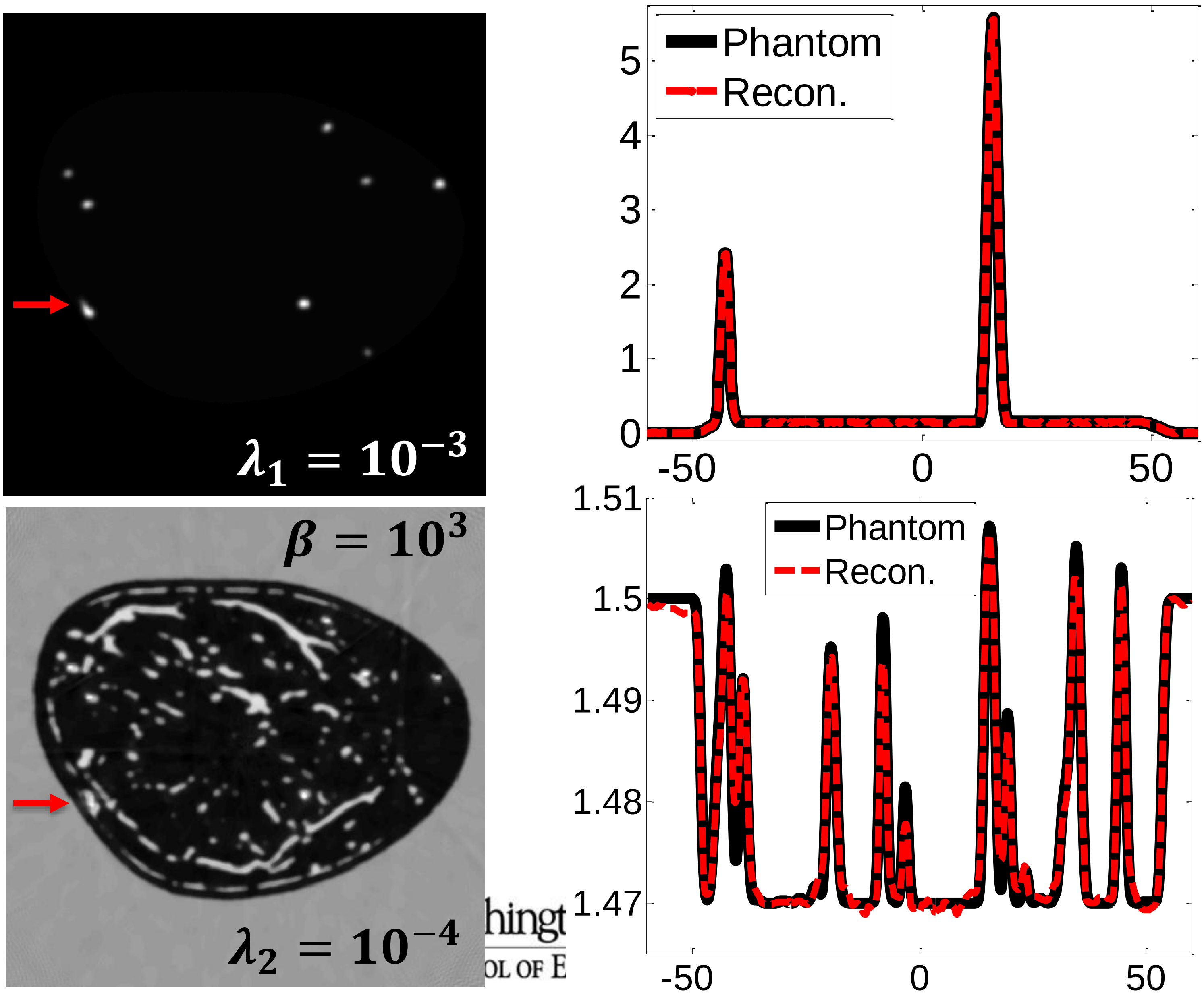

Comparison of the reconstructed sound speeds (16 views)

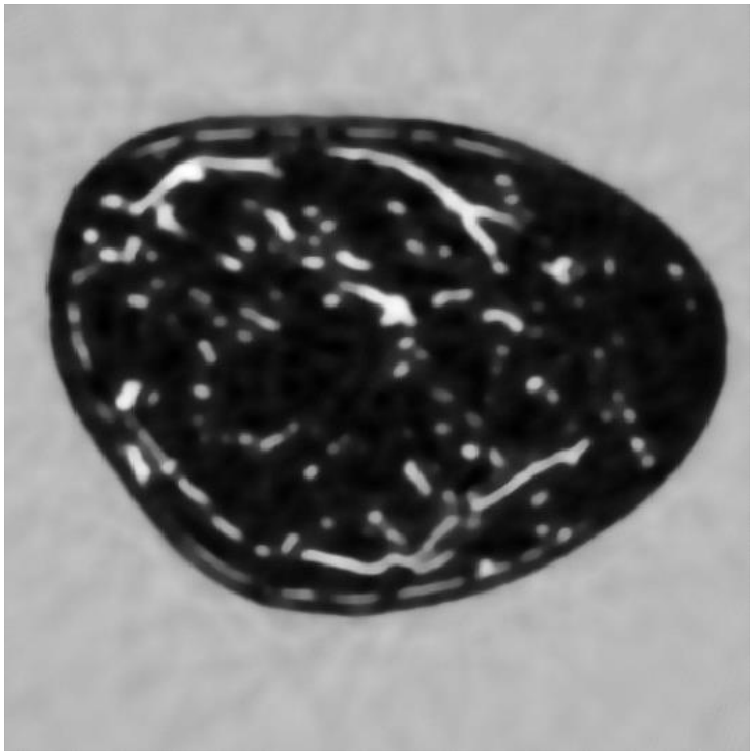

USCT only

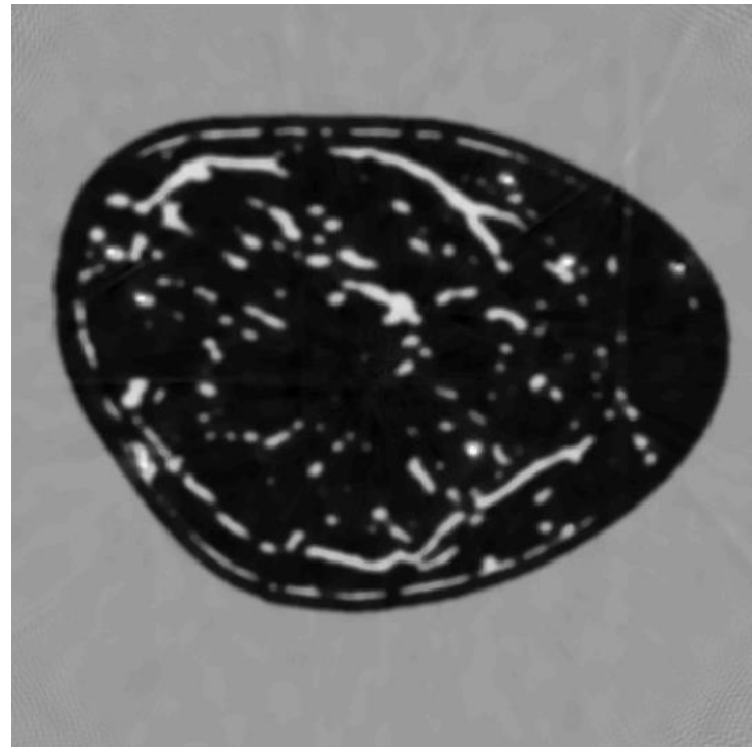

Joint Recon.

Comparison of reconstructed sound speeds (16 views)

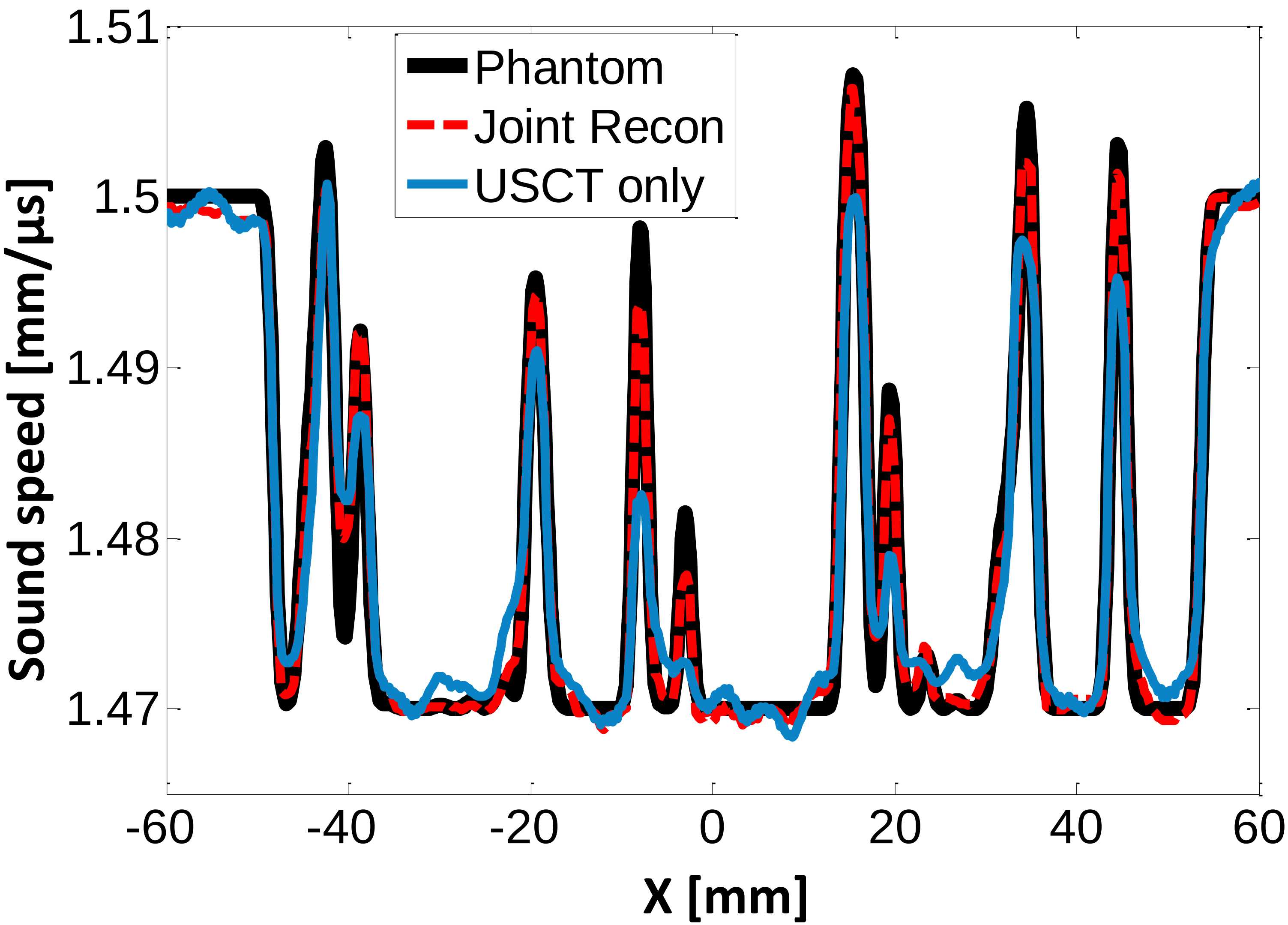

Washington University in St. Louis
School of Engineering & Applied Science

Comparison of the reconstructed sound speeds (8 views)

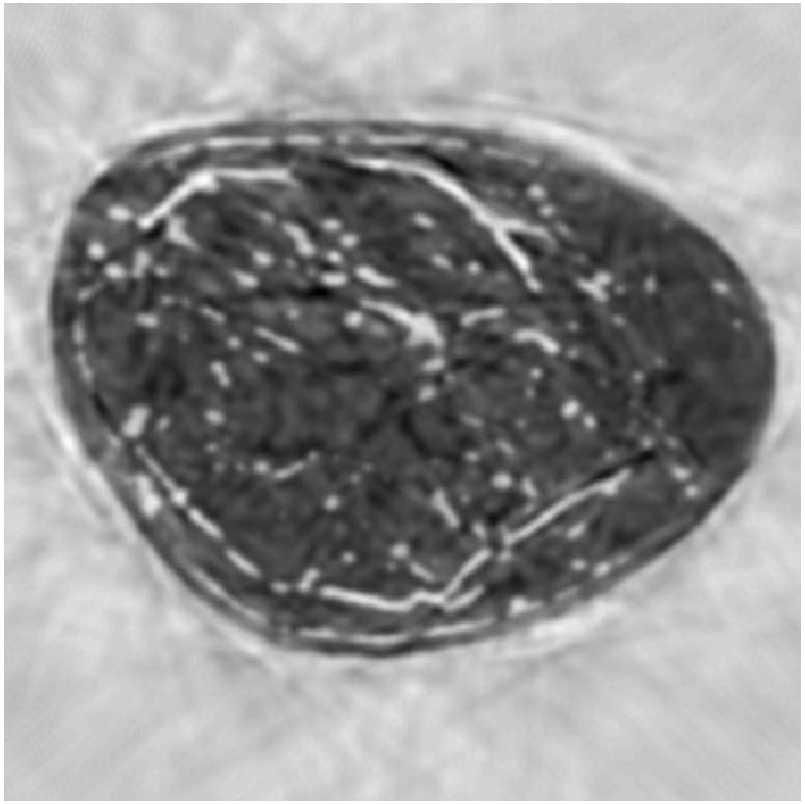

USCT only

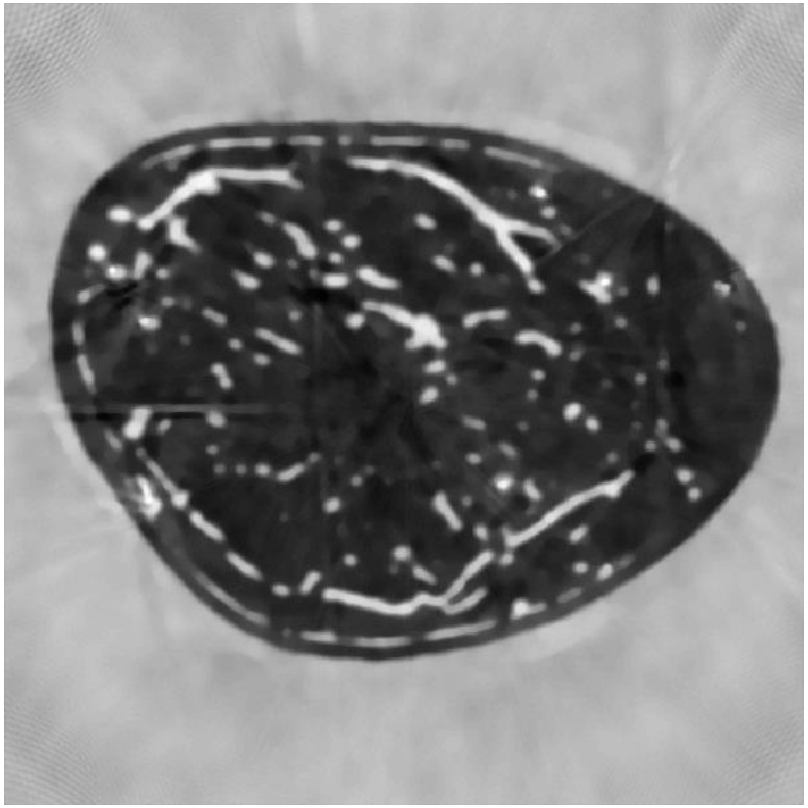

Joint Recon.

Washington University in St. Louis
School of Engineering & Applied Science

Comparison of reconstructed sound speeds (8 views)

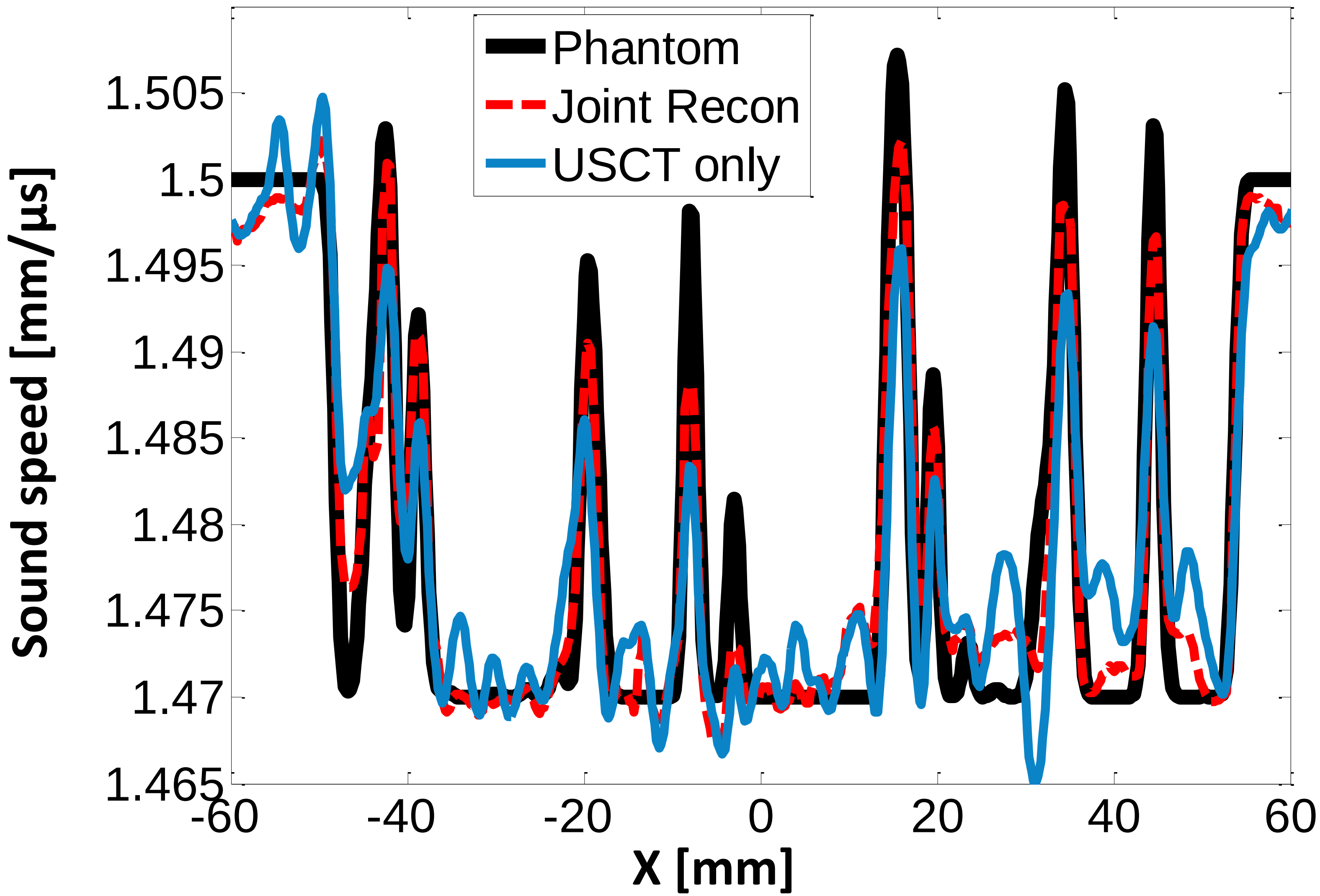

Washington University in St. Louis
School of Engineering & Applied Science

Summary

- Knowledge of the sound speed is needed for accurate reconstruction of the initial pressure distribution
- The sound speed and initial pressure distributions cannot both be stably recovered from PACT measurements alone
- Additional USCT measurements can help stabilize this joint reconstruction problem
- Acoustic information in the PACT data reduces the number of USCT views needed for accurate estimation of the sound speed

Future Work

- These studies are still preliminary
- Need to investigate the impact of noise
- Need to investigate the impact of model error (e.g. ignoring attenuation, transducer properties)

Acknowledgments

- Special thanks to:
  - » Dr. Kun Wang
  - » Dr. Chao Huang
  - » Dr. Mark Anastasio
  - » All members of the lab

- Funding sources
  - » NIH awards EB010049, CA1744601, EB01696031
  - » DOD award US ARMY W81XWH-13-1-0233

http://anastasio.wustl.edu/

Washington University in St.Louis
SCHOOL OF ENGINEERING & APPLIED SCIENCE

References

H. Avron and S. Toledo, J. of ACM, 58(2): 8:1-8:17 (2011).

A. Beck and M. Teboulle, IEEE Trans. Med. Imaging, 18(11): 2419-2434 (2009).

O. Bousquet and L. Bottou, Adv. in Neural Info. Processing Systems, 161–68 (2008).

E. Haber et. al., SIAM J. Optimiz., 22(3), P739-757 (2012).

A. Hormati, et al., Proc. SPIE, 7629: 76290L (2010).

K. Hickmann, Ph.D. thesis, Oregon State University (2010).

C. Huang, et al., IEEE Trans. Med. Imaging, 6(32): 1097-1110 (2003).

C. Huang, et al., IEEE Trans. Comp. Imaging, 2(2): 136-149 (2016).

M. Hutchinson, Comm. in Stat., Sim. and Comp., (18):1059–1076 (1989).

H. Jiang, et al., JASA, 23(4): 878-888 (2006).

X. Jin and L.V. Wang, Phys. Med. Biol., 51: 6437-6448 (2006).

J. Jose, et al., Optics Express 19(3): 2093-2104 (2011).

J. Jose, et al., Med. Physics, 39(12): 7262-7271 (2012).

A. Kirsch and O. Scherzer, SIAM J. Appl. Math., 72(5): 1508-1523 (2012).

T. van Leeuwen, et al., Inter. J. of Geophysics, 2011: 1–18 (2011).

Y. Lou, et al., Proc. SPIE, 9708: 97084O (2016).

S. Manohar, et al., Appl. Phys. Letters, 91: 131911 (2007).

References

T. Matthews, et al., Proc. SPIE, 9323: 93233A (2015).

J. Nocedal, Math. Comp., 35(151): 773-782 (1980).

R. Plessix, Geophysical J. Int. 167(2), 495–503 (2006).

P. Stefanov and G. Uhlmann, Inv. Problems and Imaging, 7(4): 1367-1377 (2013a).

P. Stefanov and G. Uhlmann, Trans. Amer. Math. Soc., 365(11): 5737-5758 (2013b).

M. Tabei et al., JASA, 111(1): 53-63 (2002).

K. Wang, et al., IEEE Trans. UFFC, 62(3): 475-494 (2015).

J. Wiskin, et al., JASA, 131(5): 3802-3813 (2012).

J. Xia, et al., Optics Letters, 38(16): 3140-3143 (2013).

Y. Xu and L.V. Wang, IEEE Trans. UFFC, 50(9): 1134-1146 (2003).

Z. Yuan, et al., Optics Express, 14(15): 6749-6754 (2006).

J. Zhang, et al., Proc. SPIE, 6856 (2008).

Z. Zhang, et al., Proc. SPIE, 8320: 832003 (2012).

BACKUP SLIDES

Reconstructed sound speed (Impact of initial guess)

Bent-ray

[Hormati 2010]

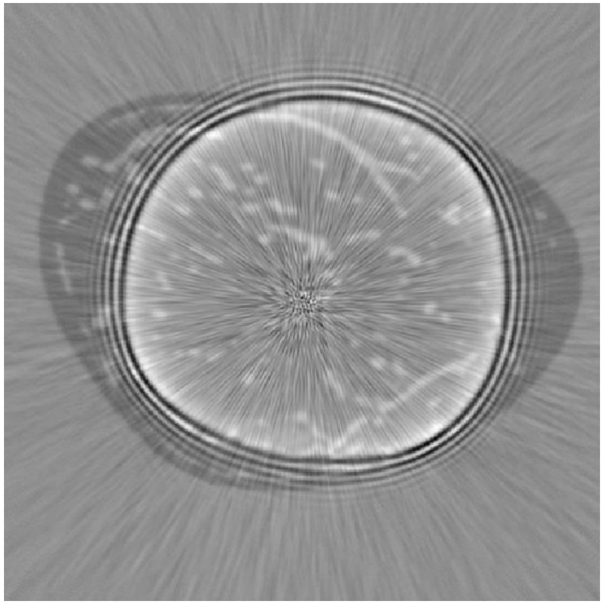

Const. init. guess

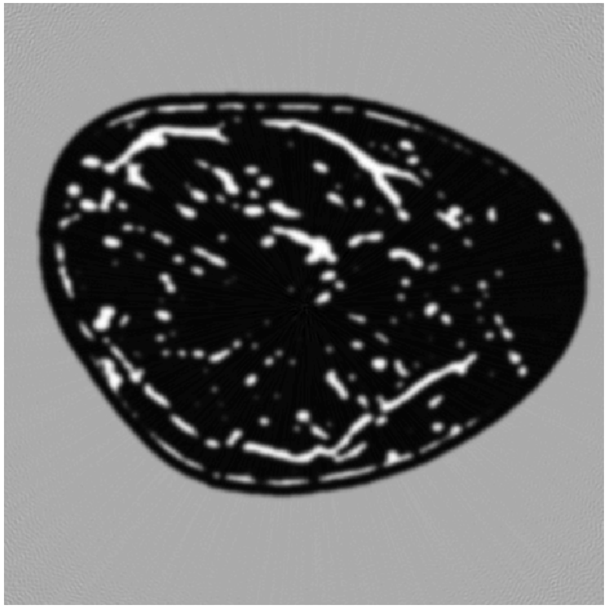

Bent-ray init. guess

Gradient of data fidelity term w.r.t. sound speed

To compute the gradient, the adjoint wavefield must be calculated for each emitter

$$\underline{\mathbf{q}_v} = \frac{1}{4\pi}\mathbf{H}_c \boldsymbol{\tau}_v$$

where

Adjoint wavefield

$$\boldsymbol{\tau}_v = \mathbf{M}^{\dagger}\left(\mathbf{M}\mathbf{H}_c\mathbf{s}_v - \underline{\mathbf{g}_v}\right)$$

is simply the time-reversed error between our estimated pressured and the measured pressure.

$$\mathbf{J}_v \equiv \nabla\left(\frac{1}{2}\|\underline{\mathbf{g}_v} - \mathbf{M}\mathbf{H}_c\mathbf{s}_v\|^2\right)$$

T: number of time points

Δt: time step

$$\underline{[\mathbf{J}_v]_n} = \frac{1}{[\mathbf{c}]_n^3}\sum_{t=1}^{T-2}[\mathbf{q}_v]_{nT+(T-t)}\frac{[\mathbf{p}_v]_{nT+t+1} - [\mathbf{p}_v]_{nT+t} + [\mathbf{p}_v]_{nT+t-1}}{\Delta t}$$

Gradient at nth pixel

R. Plessix, *Geophysical J. Int.* 167(2), 495–503 (2006).
K. Wang, et al. *IEEE UFFC* 62(3), 475-94 (2015).

Choice of encoding vector

- Relate data fidelity term to randomized trace estimation – want to estimate tr(A), but only have access to estimates of the form

$$Y = \frac{1}{K}\sum_{k=0}^{K-1} \mathbf{w}_k^\dagger \mathbf{A} \mathbf{w}_k$$

- Notice that our original cost function can be rewritten as

$$\mathcal{F}(\mathbf{c}) = \|\underline{\mathbf{g}} - \mathbf{M}\mathbf{H}_c\mathbf{s}\|_F^2 = tr\left(\left(\underline{\mathbf{g}} - \mathbf{M}\mathbf{H}_c\mathbf{s}\right)^\dagger\left(\underline{\mathbf{g}} - \mathbf{M}\mathbf{H}_c\mathbf{s}\right)\right)$$

where

$$\underline{\mathbf{g}} = \mathrm{cat}\left(\{\underline{\mathbf{g}_v}\}\right) \quad \mathbf{s} = \mathrm{cat}\left(\{\mathbf{s}_v\}\right)$$ (combine all views)

- Let $\mathbf{A} \equiv \left(\underline{\mathbf{g}} - \mathbf{M}\mathbf{H}_c\mathbf{s}\right)^\dagger\left(\underline{\mathbf{g}} - \mathbf{M}\mathbf{H}_c\mathbf{s}\right)$. Then evaluating the cost function is equivalent to finding the trace of A.

T. Van Leeuwen, et al. *Inter. J. of Geophysics* 2011: 1–18.

Washington University in St. Louis
School of Engineering & Applied Science

Choice of encoding vector

- Criteria for evaluating a trace estimator Y
  - » Variance of one sample
  - » Bounds on number of samples for given error:

$$\Pr\left(\left|Y - tr\left(\mathbf{A}\right)\right| \leq \epsilon \left|tr\left(\mathbf{A}\right)\right|\right) \geq 1 - \delta$$

A is an nxn symmetric positive semi-definite matrix

Estimator	Variance of one sample	Bound on # samples for (ϵ, δ)-approx.	Random bits per sample
Gaussian	$2\|\|A\|\|_F$	$\mathbf{20\epsilon^{-2}\ln\left(\frac{2}{\delta}\right)}$	$O(n)$
Rachemacher ($\Pr(w_i = \pm 1) = \frac{1}{2}$)	$\mathbf{2\left(\|\|A\|\|_F^2 - \sum_{i=1}^{n} A_{ii}^2\right)}$	$6\epsilon^{-2}\ln\left(2\frac{rank(A)}{\delta}\right)$	$O(n)$
DFT, Hadamard	---	$8\epsilon^{-2}\ln\left(\frac{4n^2}{\delta}\right)\ln\left(\frac{4}{\delta}\right)$	$O(\log n)$

M. Hutchinson. Comm. in Stat., Sim. and Comp., (18):1059–1076, 1989.

Washington University in St. Louis
School of Engineering & Applied Science

H. Avron and S. Toledo. J. of ACM. 58(3): 8:1-8:17 (2011).

Speed-of-sound reconstruction in USCT

- Straight-ray model
  - » Filtered back-projection (FBP) algorithm
- Bent-ray model
  - » Ray-tracing method
  - » Rayless method
    (e.g., adjoint state method)
- Linearized wave equation model
  - » Diffraction tomography
  - » Distorted Born iterative methods
- <u>Full-wave equation model</u>
  - » Waveform inversion method
  (Most comprehensive)

A.C. Kak and M. Slaney, [Principles of Computerized Tomographic Imaging], IEEE Press, 1988

Hormati et.al. Proc. SPIE 7629, (2010)
C. Li, Ultrasound Med. Biol. 35(10), 1615 (2009)

Fatima Anis et.al., Proc. SPIE 8943, (2014)

F. Simonetti et.al., Appl. Phys. Lett. 95, 067904 (2009)

J. Hesford and W. C. Chew, J. Acoust. Soc. Am., 128(2), 679 (2010)

C. Li et. al., Proc. SPIE, 9040, (2014)

Standard waveform inversion method

- Calculation of the gradient requires 2V wave equation solver runs - Computationally burdensome.

$$\mathbf{J} = \mathbf{0}$$

$$\textbf{for } v := 0 \textbf{ to } V - 1 \textbf{ do}$$

$$\mathbf{p}_v = \underline{\mathbf{H}_c}\mathbf{s}_v$$ Simulate the pressure

$$\mathbf{q}_v = \underline{\mathbf{H}_c}\boldsymbol{\tau}_v$$ Propagate residuals backward in time

$$\mathbf{J}_v = \text{calcGradient}\left(\mathbf{c}, \mathbf{p}_v, \mathbf{q}_v\right)$$

$$\mathbf{J} = \mathbf{J} + \mathbf{J}_v$$

$$\textbf{end for}$$

Implementation & Algorithm performance

Solved by stochastic optimization algorithms (Online learning algorithms)

Calculation of the gradient of ONE realization requires only 2 wave equation solver runs (in comparison to 2V).

$$\text{Choose } \mathbf{w}$$

$$\text{Compute } \mathbf{s}_w \text{ and } \underline{\mathbf{g}_w}$$

$$\mathbf{p}_w = \mathbf{H}_c \mathbf{s}_w$$

$$\mathbf{q}_w = \mathbf{H}_c \boldsymbol{\tau}_w$$

$$\mathbf{J}_w = \text{calcGradient}\left(\mathbf{c}, \mathbf{p}_w, \mathbf{q}_w\right)$$

where

$$\boldsymbol{\tau}_w = \mathbf{M}^\dagger \left(\mathbf{M}\mathbf{p}_w - \underline{\mathbf{g}_w}\right)$$

Algorithm performance

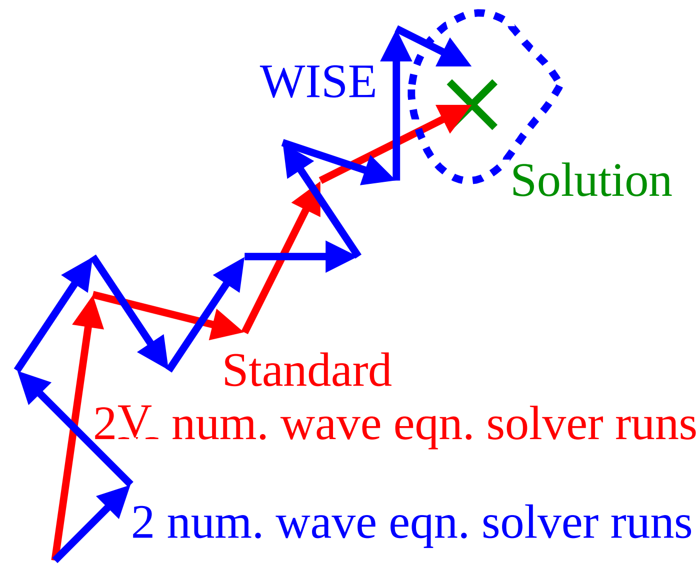

K. Wang, et al. *IEEE UFFC* 62(3), 475-94 (2015).

Washington University in St. Louis
School of Engineering & Applied Science

Intuitive interpretation of encoded source

- Replace V single shots with a super shot

- Encoded source may introduce a cross-talk, which can be mitigated through iteration with properly designed w.

- Overall computational saving if

$$K_{\text{std}} < K_{\text{wise}} \ll \mathbf{V}\ K_{\text{std}}$$

(K_{std} and K_{wise}: # iterations required for convergence)

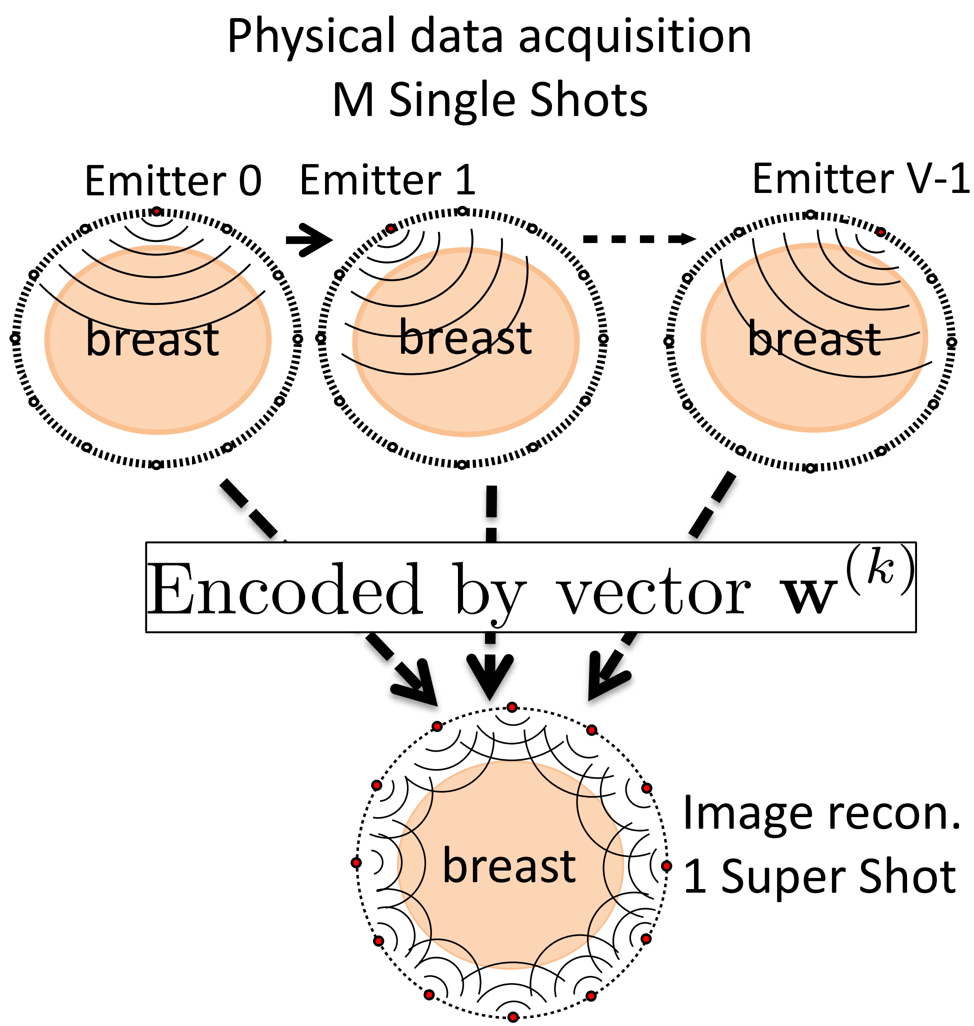

K. Wang, et al. *IEEE UFFC* 62(3), 475-94 (2015).

Washington University in St. Louis
School of Engineering & Applied Science

Theoretical convergence rates

- Gradient descent achieves linear convergence
- Stochastic gradient descent achieves sub-linear convergence

Algorithm	Cost of one iteration	Iterations to reach accuracy ε	Time to reach accuracy ε
Gradient descent	$O(V)$	$O\left(\log\frac{1}{\epsilon}\right)$	$O\left(V\log\frac{1}{\epsilon}\right)$
Stochastic gradient descent	$O(1)$	$O\left(\frac{1}{\epsilon}\right)$	$O\left(\frac{1}{\epsilon}\right)$

- However, when number of emitters is large, the time to reach a given accuracy can be much shorter in the stochastic case.

O. Bousquet and L. Bottou. *Adv. in Neural Info. Processing Systems*, 161–68, 2008.